Exergetic efficiency and CO2 intensity of hydrogen supply chain including underground storage

Baghirov, Boyukagha; Voskov, Denis; Farajzadeh, Rouhi

DOI
10.1016/j.ecmx.2024.100695

Publication date
2024

Document Version
Final published version

Published in
Energy Conversion and Management: X

Energy Conversion and Management: X 24 (2024) 100695

Contents lists available at ScienceDirect

Energy Conversion and Management: X

journal homepage: www.sciencedirect.com/journal/energy-conversion-and-management-x

Exergetic efficiency and CO_2 intensity of hydrogen supply chain including underground storage

Boyukagha Baghirov [a,*], Denis Voskov [a,b], Rouhi Farajzadeh [a,c]

[a] Department of Geoscience and Engineering, Delft University of Technology, the Netherlands
[b] Department of Energy Science and Engineering, Stanford University, USA
[c] Shell Global Solutions International, the Netherlands

ARTICLE INFO

Keywords:
Hydrogen
CO_2 intensity
Exergy Analysis
Energy Storage
CCS

ABSTRACT

Hydrogen plays a crucial role in the transition to low-carbon energy systems, especially when integrated into energy storage applications. In this study, the concept of exergy-return on exergy-investment (ERoEI) is applied to investigate the exergetic efficiency (defined as the ratio of useful exergy output to invested exergy input) and CO_2 equivalent intensity of the hydrogen supply chain, with a specific focus on the underground hydrogen storage process. Our findings reveal that the overall exergetic efficiency of the electricity-to-hydrogen-to-electricity conversion process can reach up to 25 %. Among the hydrogen production methods, green hydrogen, produced via electrolysis powered by renewable energy, exhibits the lowest CO_2 equivalent intensity. Blue hydrogen, produced from natural gas with carbon capture, can significantly reduce the carbon footprint of electricity generation, though this advantage comes at the expense of decreased exergetic efficiency. Analysis further indicates that the exergetic efficiency of underground storage components ranges from 72 % to 92 %. A substantial fraction of the exergy is lost during compression and injection of the stored hydrogen. Nevertheless, the subsurface operations contribute a minimal CO_2 emission, between 1.46–4.56 grams of equivalent CO_2 per megajoule (gr-CO_{2eq}/MJ) when powered by low-carbon energy sources. Furthermore, it is found that hydrogen loss in the reservoir, along with methane and hydrogen leak during surface operations, notably affects the overall efficiency of the storage process.

Introduction

To effectively address climate change and secure a sustainable energy future, transitioning to low carbon, particularly, renewable energy sources is essential. In 2022, fossil fuels maintained a dominant position, constituting nearly 80 % of the global energy mix, while renewables only made up about 20 % of the total energy mix [1]. However, projections indicate a significant transformation, with fossil fuel's share anticipated to decline steadily, while renewable energy sources are forecasted to surpass 50 % of total energy consumption by 2050 [1]. Despite this growth, electricity generation from renewable sources, such as wind and solar, remains inherently dependent on weather conditions and time of day, posing challenges for establishing a reliable and scalable power network. A potential solution lies in the storage of renewable electricity during peak production periods for later use [2].

Hydrogen (H_2) has emerged as a promising storage medium and energy carrier, offering the potential to decarbonize the energy sector effectively. Its capacity for long-term storage enables the utilization of excess renewable energy during periods of high demand. The high energy density of H_2 (118 MJ/kg) and clean combustion, producing only water vapor make it an ideal fuel for electricity and heat generation [3]. With the ability to be produced from renewable sources such as wind and solar power through processes like electrolysis (green H_2), hydrogen holds immense potential to facilitate the transition to a low-carbon economy. Furthermore, hydrogen produced from fossil fuels using carbon capture and storage (CCS) technology, commonly referred to as blue H_2, also contributes to the decarbonization of the energy portfolio, despite not being directly sourced from renewables [4]. However, realizing the full potential of H_2 as an energy carrier entails overcoming several challenges. Firstly, the production of hydrogen is currently energy-intensive and costly, with the majority produced from methane (CH_4) and other hydrocarbons (96 % of total produced H_2), leading to substantial greenhouse gas emissions. Only a small fraction (4 %) of H_2 is produced via low-carbon water electrolysis [5]. Moreover, the low

* Corresponding author.
E-mail address: b.baghirov@tudelft.nl (B. Baghirov).

https://doi.org/10.1016/j.ecmx.2024.100695
Received 4 June 2024; Received in revised form 28 July 2024; Accepted 21 August 2024
Available online 23 August 2024

volumetric density of hydrogen necessitates expensive pressurization or liquefaction for storage, posing economic and safety challenges. Current storage methods, primarily, in pressurized or cryogenic containers as either gas or liquid, are insufficient to meet large-scale (TWh) storage demand. Therefore, establishing cost-effective, secure, and reliable H_2 storage systems is imperative to foster the growth of a hydrogen economy [6].

Underground storage offers a viable solution for long-term and large scale H_2 storage, leveraging various global geological formations. Different types of underground reservoirs, such as solution-mined salt caverns [7–9], saline aquifers [10–12], and depleted hydrocarbon fields [13,14] have been explored as potential storage sites for hydrogen. Integrating underground storage with green and blue H_2 production contributes to achieving decarbonization targets and reducing greenhouse gas emissions in the energy industry. While green H_2 aligns directly with renewable energy sources, blue H_2 offers a dependable energy resource to complement intermittent renewables. Furthermore, existing studies and industrial practices underscore the viability and significance of integrating blue H_2 production with geological storage options to facilitate the transition toward sustainable energy and reduce carbon emissions in the energy industry [4,15–17]. However, despite its potential, underground H_2 storage systems have not undergone a comprehensive evaluation concerning their thermodynamic efficiency and environmental impact within the entire H_2 supply chain, including underground storage options.

Several studies in the literature have conducted thermodynamic and environmental assessments of H_2 production and storage systems. Ozcan et al. [18] conducted an exergy analysis of a solar-based H_2 production and storage system, yielding overall energy and exergy efficiencies of 16.31 % and 17.6 %, respectively. The solar field accounted for the largest portion of the total exergy investment, approximately 64 %. Calderon et al.[19] proposed a system integrating photovoltaic (PV) and wind technologies with H_2 storage to meet the electrical energy demands of Badajoz, Spain. They found that PV modules in Badajoz exhibited a low exergy efficiency of 8.39 %. Khosravi et al. [20] investigated energy, exergy, and economic analyses for renewable hybrid energy systems utilizing H_2 storage, suitable for remote areas, achieving average energy and exergy efficiencies of 12 % and 16 %, respectively. The PV system exhibited the highest exergy destruction at approximately 65 %. Al-Zareer et al. [21] assessed the efficiency of two compressed H_2 storage systems, estimating overall exergy efficiencies of 92.9 % and 96.1 % for the first and second models, respectively. Neelis et al. [22] conducted a life-cycle analysis of H_2 production and storage systems for automotive applications using eight fuel chains. Compressed H_2 storage systems demonstrated the highest exergetic efficiency, while liquid H_2 systems exhibited lower exergetic efficiency due to the significant exergy requirements for liquefaction. Farajzadeh et al. [23] calculated the exergetic efficiency and CO_2 intensity of underground bio-methanation processes using renewable H_2 for electricity and heat generation. The biomethanation process achieved maximum exergetic efficiencies of 15–33 % for electricity and 36–47 % for heat generation, with H_2 production being the primary exergy consumer in both applications. Pérez et al. [24] compared the conversion efficiency of H_2 to renewable electricity within underground energy storage systems (adiabatic compressed air storage, hydrogen storage, and methanation). The conversion efficiency of H_2 storage in salt caverns was calculated to be 43–48 %.

Furthermore, from an environmental perspective, our analysis primarily focuses on the CO_2 footprint of hydrogen production and storage systems. Bhandari et al. [25] conducted a comprehensive analysis of 21 studies examining the life cycle assessment (LCA) of various H_2 production methods, focusing on ecological considerations. They found a consistent global warming potential (GWP) of 0.97 kg CO_{2eq}/kg H_2 for wind-based electrolysis, while steam methane reforming of natural gas showed GWP values ranging from 8.9 to 12.9 kg CO_{2eq}/kg H_2. Sebastian et al. [26] examined the life-cycle greenhouse gas emissions of H_2 production via different CH_4 decomposition methods (plasma, molten metal, and thermal gas), and found that the plasma system using renewable electricity generated the lowest emissions, with 43 g CO_{2eq}/MJ. G. Kubilay et al [27] focused on the environmental implications of different hydrogen storage technologies. Their findings indicated that liquid hydrogen storage resulted in the lowest emissions, averaging 3.5 kg CO_{2eq} per kg of stored H_2, whereas metal hydride storage tanks exhibited the highest emissions, reaching 113.6 kg CO_{2eq}. Bicer et al. [28] evaluated four green ammonia production methods and estimated greenhouse gas emissions for each option. Municipal waste sources had the lowest CO_2 equivalent emissions (0.34 kg CO_{2eq}). Other studies explored different H_2 production methods in terms of production cost and CO_2 emissions [29–32].

In summary, various studies have focused on the thermodynamic or environmental analysis of H_2 production and storage systems, separately. However, while a thermodynamically optimized system might excel in one aspect, it might not be optimal in terms of environmental considerations, or vice versa [23,33,34]. Despite the potential for optimizing systems based on thermodynamic or environmental criteria alone, a holistic approach is necessary for viable engineering solutions. Thus, it is imperative to simultaneously consider all or a subset of these criteria to identify a more optimal solution [23,33,34]. A key feature of our study is the integration of thermodynamic (exergy) and environmental (CO_2 intensity) analyses into a unified framework. Furthermore, there exists a substantial gap in the literature concerning the evaluation of thermodynamic efficiency or exergetic efficiency, and particularly CO_2 intensity throughout the full cycle of the H_2 supply chain, including the option of underground hydrogen storage (UHS). Therefore, our study aims to bridge this gap by developing exergy-based method to define the exergetic efficiency and CO_2 intensity (grams of CO_2 per MJ of electricity) of the full life-cycle H_2 supply chain with encompassing underground storage.

Exergy serves as a helpful metric for evaluating and comparing the sustainability of energy storage systems [35–37]. It is the maximum portion of the energy that can be converted to useful work [23,38]. Exergetic efficiency, also known as Exergy Return on Exergy Invested (ERoEI), denotes the percentage of exergy input (exergy investment) transformed into productive work (exergy return), with the remaining "lost" or "wasted" exergy attributable to irreversibilities described by the second law of thermodynamics, practically contributing to CO_2 emissions [23,39,40]. In the study, exergy analysis is done with several common H_2 production methods with high technical readiness level (TRL). The results are then compared to the case of producing electricity from CH_4, whose CO_2 has been captured. By comparing various hydrogen production (green and blue H_2) methods and calculating ERoEI and CO_2 intensity, our research offers novel insights into optimizing the H_2 supply chain and its environmental footprint. Importantly, the analysis considers CH_4 and H_2 leakage and their global warming potential in the study as well to reflect their environmental impact accurately. The results of this paper provide insights into contribution of each stage of the process on the exergetic efficiency and levelized CO_2 footprint of the H_2 supply chain, including UHS system, which can then be used for optimization purposes.

The paper is structured as follows: Initially, the H_2 supply chain and its boundaries are precisely defined for assessment. Next, the work and material streams of the system are calculated based on underlying assumptions. These data are then used to determine the ERoEI and CO_2 intensity of the UHS process with different H_2 production methods. A sensitivity analysis is performed to quantify the impact of different parameters on the results. The results are presented in two distinct sections: the first section discusses the findings of overall H_2 supply chain process, and the second part focuses exclusively on the UHS process. The paper concludes with insightful remarks summarizing the findings.

System and Methodology

Method of analysis

In this study, the method based on the concept of Exergy Return on Exergy-Investment (ERoEI) is applied to investigate the exergetic efficiency and CO_2 intensity of the H_2 supply chain for electricity application including underground storage process. The intermediate and final results of the exergy analysis serve as valuable tools for decision-makers to identify the most optimal scenario for the studied process while minimizing environmental impact [23,35,37,38]. The ERoEI is defined as

$$ERoEI = \frac{Ex_{returned}}{Ex_{invested}} \quad (1)$$

where, $Ex_{returned}$ represents the gained exergy (in MJ) from the produced fuel (H_2 and CH_4) and $Ex_{invested}$. signifies the total exergy investment in different stages of the process. Theoretically, ERoEI can range from 0 to $+\infty$. For the system considered in this study, eq. (1) is expanded to:

$$ERoEI = \frac{Ex^{ch}_{H_2} \times \eta}{Ex_{H_2prod.} + Ex_{tran.} + Ex_{UHS} + Ex_{end\_use}} \quad (2)$$

Here, the returned exergy is the chemical exergy of H_2 ($Ex^{ch}_{H_2}$) discounted by the efficiency (η) of the fuel cell. The invested exergy includes exergy requirement for H_2 production ($Ex_{H_2prod.}$), transportation ($Ex_{tran.}$), underground storage (Ex_{UHS}), and the end-use application streams (Ex_{end_use}). To perform the exergy analysis, the material ($Ex_{returned}$) and work ($Ex_{invested}$) streams of the system depicted in Fig. 1 are elaborated in more detail [23,38,40].

After estimating the consumed exergy, the CO_2 intensity of the process can be calculated. The carbon intensity is defined as the mass of CO_2 released per unit of energy (gr-CO_2/MJ). To estimate the carbon intensity, the invested exergy of the system is multiplied by the specific carbon emission of the energy resources (Table 1) [23]. The specific CO_2 emission of CH_4 and wind power are considered 55 and 7 gr-CO_2/MJe, respectively [41,42]. To provide a reliable quantitative analysis, the levelized CO_2 equivalent emission is calculated by considering CH_4 (extraction and transportation to H_2 production side) and H_2 leakages (throughout the entire supply chain, including H_2 production, transportation, underground storage, and end-use application) and their global warming potential (GWP) for a selected period of 100 years, i.e.,

$$CO_{2eq.int} = \frac{Ex_{invested} \times W + M \times L \times GWP}{Ex_{returned}} \quad (3)$$

Table 1
Main input values used for calculating CO_{2eq} intensity. The ''blue'' refers to H_2 production from methane, whose associated CO_2 has been captured.

Input	Value	References
CH_4 consumption (blue H_2 production option)	3–3.8 kg/kg H_2	[30,43]
H_2 consumption	1 kg	–
Leak rate during CH_4 consumption (mass fraction)	0–1.5 %	[44–48]
Leak rate during H_2 consumption (mass fraction)	3.5–9 %	[49]
GWP-100 of CH_4	28	[50]
GWP-100 value of H_2	12	[51,52]
Specific CO_2 emission of CH_4	55 gr-CO_2/MJe	[41]
Specific CO_2 emission of wind power	7 gr-CO_2/MJe	[42]

where, W represents the specific carbon intensity of energy source (gr-CO_2/MJ), M denotes the mass of the utilized fuel (including CH_4 consumption in the hydrogen production process and H_2 consumption across the full H_2 chain), and L shows the leaked mass fraction of gases (H_2 or CH_4) occurring at various stages of the process.

System definition

Fig. 1 depicts the main components of a H_2 supply chain including hydrogen storage process. The overall system consists of the H_2 production, transportation, underground storage, and end-use application subsystems. For this study, the system conditions are modelled based on a candidate depleted gas reservoir. The initial stage involves H_2 production through various methods outlined in Table 2. For blue options, steam methane reforming (SMR), autothermal reforming (ATR), and partial oxidation (POX) methods are explored due to their widespread usage and high technical readiness levels (TRL) [30,53]. Water electrolysis, utilizing electricity sourced from low-carbon sources (in this case, windmills), is chosen for green H_2 production. The required water undergoes desalination and treatment before entering the electrolysis unit. It is assumed that the water source is near the plant, with negligible production and transportation exergy requirements.

Afterwards, the produced H_2 is compressed to the necessary pipeline pressure, transported, and stored in a gas reservoir. Since the produced gas stream contains native reservoir gas (assumed to be pure CH_4) along with H_2, separation from other gases is necessary before final use. Regarding the produced CH_4 stream, two scenarios are considered: In Scenario 1, the produced CH_4 is reinjected back into the reservoir, whereas in Scenario 2, CH_4 is exported to a near-by power plant to generate electricity. The produced CO_2 from the power plant is captured and stored in a near-by storage site. The exported H_2 is further purified

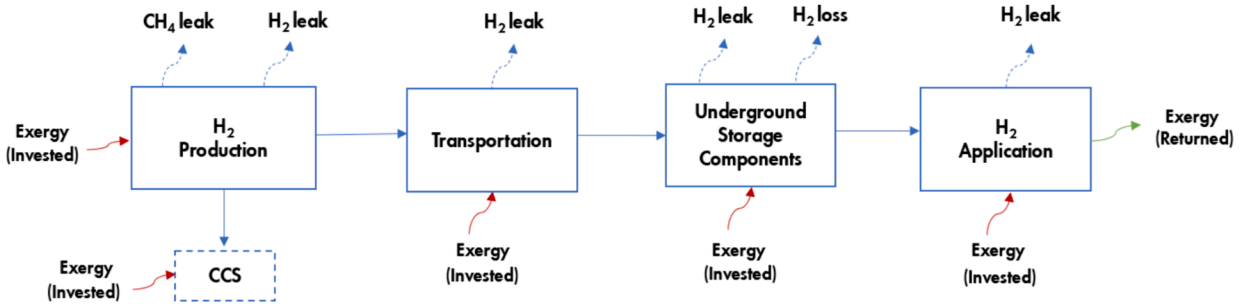

Fig. 1. Schematic view of the system boundary and main components for the full H_2 supply chain, including H_2 production, transportation, underground storage, and end-use application.

Table 2
Exergy investment in the form of heat and electricity for different H_2 production methods. CCS stands for Carbon Capture and Storage. The final exergy consumption is equal to sum of electricity and heat demand of each production method.

H_2 production methods	Abbreviation	Invested exergy (MJh/kg-H_2)	Invested exergy (MJe/kg-H_2)	Total invested exergy (MJ/kg-H_2)	References
Steam methane reforming with CCS	SMR+CCS	151–215	20–81	171–296	[30,54,55]
Auto-thermal reforming with CCS	ATR+CCS	150–185	34–110	184–295	[54,55]
Partial Oxidation with CCS	POX+CCS	139–209	26–119	165–328	[53]
Electrolysis	–	–	169–252	169–252	[64–67].

for generating electricity in fuel cells. Fig. 1: Schematic view of the system boundary and main components for the full H_2 supply chain, including H_2 production, transportation, underground storage, and end-use application.

Additionally, the following assumptions are applied in the calculations:

- The outlet pressure of the produced H_2 is 15 bar after the electrolysis process, 30 bar after the SMR, ATR, and 50 bar after the POX processes [30,53–55].
- Transportation pressure of H_2 is assumed to be 50 bar.
- The pressure of the gas reservoir is 350 bar.
- The distance from H_2 production site to the reservoir is 300 km.
- The transportation distance from the reservoir to the H_2 end-use application is 30 km.
- The gas power plant is positioned close to the reservoir (~20 km).
- The distance between CO_2 capture and storage facilities is 50 km.
- The export pressure of CH_4 is regulated at 50 bar.
- CH_4 is recompressed after separation from 50 bar to the reservoir pressure.
- 3–18 % H_2 loss [56] is considered in the reservoir due to mixing, structural trapping, solubility, biochemical and geochemical conversion processes.
- 3.5–9 % H_2 [49] and 0–1.5 % CH_4 [44–48] leakage rates are assumed in overall surface operations.
- For the system considered in this study, the main produced fuels are H_2 and CH_4, with the chemical exergy values of 118 MJ/kg and 51.8 MJ/kg, respectively [57].

In the following, different stages of the system are explained in more details.

Hydrogen Production. In this work, blue (SMR+CCS, ATR+CCS, POX+CCS) and green (water electrolysis using a low carbon power source) methods are considered as H_2 production technologies. The so-called grey option is currently the most common method for producing H_2, usually produced from the natural gas by reforming or oxidation process but without collecting the generated greenhouse gases [54,55]. In the blue H_2 option, the produced CO_2 is captured and stored in geological formations or utilized as feedstock in other processes. However, the addition of CCS stage to the process increases its energy requirements [54,55]. The magnitude of the exergy required to separate CO_2 from a gas mixture depends on its concentration or partial molar volume. Typically, monoethanolamine (MEA) solvent is used in fossil-fueled power plants to absorb CO_2 from flue gas streams with high capture efficiency (80–95 %) [40,53–55]. The required exergy with MEA-based method for capturing CO_2 can vary between 2.5–6 MJe/kg CO_2 [37,58,59]. It is important to realize that when the energy source of the CCS stage is not zero carbon, additional CO_2 is produced during the process [54,55].

In contrast to the SMR method, production of H_2 from the ATR and POX processes requires 3.2–6.6 kg of pure oxygen (O_2) per kg of H_2, thereby increasing the invested exergy for H_2 production from these methods [54,55]. The air separation unit (ASU) produces O_2 using the cryogenic distillation method and uses electricity as the primary energy input, necessitating 0.9–5.1 MJe/kg-O_2 [53]. The O_2 demand for the ATR and the POX options rises significantly when a CO_2 capturing unit is added to the system, since more natural gas and, by extension, O_2 are required by the power generating system to meet the exergy demand of CO_2 separation [54,55]. Furthermore, it is worth mentioning that both oxidation and reforming processes require 3–3.8 kg of CH_4 as feedstock per kg H_2 production, and that the CH_4 extraction requires 3–8 MJ of exergy per kg [23,30,43].

The exergy investment for production of H_2 from water electrolysis is 169–252 MJe/kg-H_2. The carbon footprint of this method largely hinges on the electricity source powering the electrolysis. These values also encompass water desalination and treatment, which involve various operations such as fine screening, coagulation-flocculation, filtration, and desalination, depending on the selected water source for the electrolysis process [60,61]. H_2 production from water electrolysis consumes from 10.0 to 22 kg water per kg of H_2. This study focuses on using seawater for electrolysis, which demands 1–6 MJe/kg-H_2, factoring in the energy for desalination and purification processes [60–63]. For the purpose of our analysis, the electricity for green H_2 production is sourced from wind turbines, associated with a CO_2 intensity of 1–3 kg-CO_2/kg [64–67].

Table 2 provides the magnitude of required exergy in the form of heat (MJh) and electricity (MJe) for different H_2 production methods.

Transportation. The transportation phase involves initially compressing H_2 and transporting it to the field site via a pipeline. For the case considered here, H_2 is initially compressed to 50 bar and transported by pipeline to the storage site located 300 km away from the production site. The exergy requirement for the initial compression varies depending on the outlet pressure of the H_2 production method. For example, the outlet pressure of the POX method is already at 50 bar and therefore it does not require further compression at this stage [53]. Compression is assumed to be an isentropic (adiabatic) process, which means that the entropy of the streams remains constant. CoolProp is used to perform the thermodynamic calculations [68].

To compute the practical exergy, expressed as:

$$Ex_{comp}^{prac} = \frac{Ex_{comp}^{th}}{\eta_{comp}\eta_d} = \frac{H_2(S_1(T_1,P_1),P_2) - H_1(S_1(T_1,P_1),P_1)}{\eta_{comp}\eta_d} \quad (4)$$

the efficiencies of the compressor (0.50–0.90) [69,70] and the electrical drive (0.8–0.9) [23,71] are considered in Eq. (4) [40]. It is assumed that all required electricity is supplied from a low-carbon renewable (wind) source. The efficiency of the wind power plants is in the range of 0.30–0.55 [72]; however, this is not considered in the calculations. The practical exergy investment for initial compression is provided in Table 3.

Table 3
Calculated compression exergy for transportation and injection of H_2.

Work Stream	Theoretical Exergy (MJe/kg H_2)	Practical Exergy (MJe/kg H_2)
Transportation Compression (from 15 to 50 bar) Electrolysis output	1.8	2.2–4.5
Transportation Compression (from 30 to 50 bar) SMR, ATR output	0.7	0.86–1.75
Injection Compression (from 50 to 350 bar)	3.0	3.7–7.5

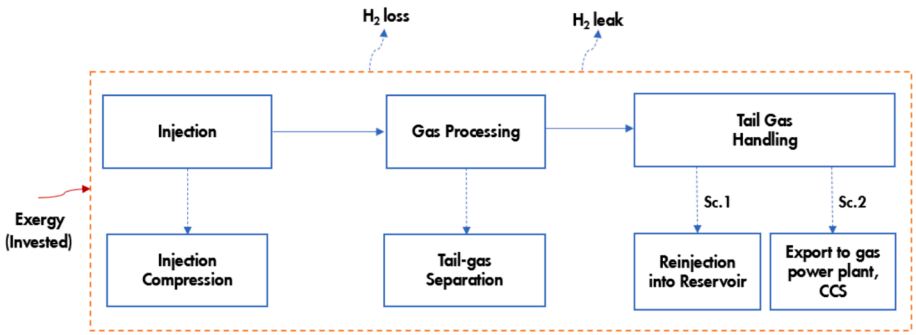

Fig. 2. Schematic overview of the underground hydrogen storage components. The blue dashed lines highlight subcomponents of the underground storage components. (For interpretation of the references to colour in this figure legend, the reader is referred to the web version of this article.)

Additionally, during transportation, a pressure drop of 0.15–0.30 bar/km and an exergy consumption of 1.44–3.96 MJe/kg H_2 for pipeline transport are considered [73,74].

Underground Hydrogen Storage Components (UHS). A UHS system typically consists of three main parts: injection, gas processing, and tail gas handling parts, as shown in Fig. 2.

Injection Component. In this stage, H_2 is recompressed to a pressure of 350 bar, which corresponds to the reservoir pressure, and subsequently injected into the reservoir. The compression exergy values are provided in Table 3.

Gas processing. During the storage period, H_2 mixes with in-situ gases in the gas reservoir. Therefore, it is crucial to separate H_2 from the produced tail gas before transferring it to next stage. The gas processing segment of the UHS process involves separating H_2 from the produced fluids (mixture of gases and possibly water), and transporting it to the application side. The chosen technology for H_2 separation from the H_2/CH_4 mixture is the pressure swing adsorption (PSA) method. The exergy requirement for gas separation is indicated in Table 4. It is assumed that the produced gas mixture is mainly composed of H_2 and CH_4 with proportion of 85–100 % H_2 and 0–15 % CH_4 in-line with some simulation and field results [56]. In addition, it is assumed that H_2 end-use application is located close to the gas field (~30 km). Therefore, the exergy investment in this transportation stage can be neglected.

Tail gas handling. The separated tail gas, primarily consisting of methane (CH_4), is managed through either reinjection into the reservoir or exportation to a power plant for electricity production. For reinjection (Scenario 1), the exergy cost of compressing and injecting CH_4 is calculated to range 0.51–1.0 MJe/kg CH_4, as detailed in Table 4. Alternatively, in the Scenario 2, where CH_4 (which may be mixed with H_2) is exported to a power plant, it is essential to also capture and transport CO_2 emissions generated during electricity production (refer to Table 4 for specifics).

H_2 loss in the reservoir. During the storage period of H_2 in reservoirs, a fraction of the injected H_2 may be lost due to various factors such as the complex geology of the reservoir, lateral movements, dispersion and mixing with in-situ gas, dissolution in water, and biochemical and geochemical conversion processes. Studies indicate that the lost fraction of H_2 could range between 3–18 % [56].

Table 4 provides the main exergy investments of the subsurface components of the UHS system depicted in Fig. 2.

Table 4
Summary of the exergy requirements for the work streams of the UHS system depicted in Fig. 2.

Underground Storage Components	Practical exergy Investments [MJe/kg gas]	References
Injection	3.7–7.5	[68]
Gas Processing	3–6.9	[75,76]
Tail gas handling (Sc.1)	0.51–1	[68]
Tail gas handling (Sc.2)	2.5–6	[37,58,59]

H_2 to Electricity. Fuel cells are devices that directly convert the chemical exergy of H_2 into electricity. The only byproduct of a perfect hydrogen–oxygen fuel cell is water, although a portion of the input exergy is lost as heat during the process. The efficiency of fuel cells depends on various factors including the type of reactants, the electrolyte used, and the temperature of the reactants [77,78]. Currently, H_2 fuel cells have a conversion efficiency ranging from 40-60 % [79]. Following the gas-processing stage, there may still be some contaminants present in the transported gas, which could be acceptable within the pipeline. However, for electricity generation in H_2 fuel cells, H_2 needs to undergo further treatment to ensure its purity exceeds 99 % [78]. Various methods, including chemical and physical absorption, adsorption, pressure swing adsorption (PSA), and polymer membrane technology, can be employed for the purification process [77]. In the analysis, membrane-based purification technology is considered due to its superior recovery capability, with a required exergy of 10.8–22.1 MJe/kg-H_2 [80].

Fugitive CH_4 and H_2 emissions

CH_4 leakage. Methane is a highly potent greenhouse gas, emitting approximately 28 times as much warming as CO_2 over a 100-year time frame following a pulsed emission [50]. Achieving leak-free production and utilization of natural gas in industry poses significant challenges. Especially, both oxidation and reforming processes require 3–3.8 kg CH_4 per kg H_2 production [30,43]. OGCI (Oil and Gas Climate Initiative) member companies in the energy sector have committed to a 2025 target intensity of well below 0.20 %, with an aim to achieve near zero methane emissions by 2030 [48]. However, the measurement of methane emissions is characterized by significant uncertainty and shows large variations depending on the specific kind of fossil fuel production, such as shale oil and gas, conventional oil and gas, oil sands. The observed disparity exists in several worldwide locations, where the complex characteristics of each production process contribute to the difficulty of measuring emissions. In this study, we assume 0–1.5 % methane leakage rate for the processes consuming CH_4. Nevertheless, certain regions exhibit emissions that may extend up to 3 % [44–48].

H_2 leakage. H_2 is an indirect greenhouse gas that interacts with tropospheric hydroxyl radicals, influencing the distribution of CH_4 and ozone in the atmosphere. Moreover, it enhances the stratospheric

Table 5
H_2 leak rate (%) in various stages of the system shown in Fig. 1.

Process	Leak Rate (%)	Impacted stage in Fig. 1	References
Blue H_2 Production	1–1.5	H_2 Production	[49]
Green H_2 Production	2–4	H_2 Production	[49]
Compression, Transportation and Injection	1–2	UHS and Transportation	[49]
H_2 End Use	1.5–3	H_2 Application	[49]

concentration of water vapor, contributing to warming by hindering outgoing infrared radiation [46,81]. According to research data from Columbia University's Energy Center, the full implementation of the H_2 supply chain is associated with H_2 leakage rates ranging between 3.5–9 % throughout various stages, including production, transportation, subsurface storage (compression, injection, and separation), and end-user applications [49]. H_2 leakage has a crucial impact on the exergy and carbon efficiency of the overall H_2 chain process. The leakage rates for each stage of the process are detailed in Table 5.

Results and Discussions

In this section, we will conduct a thorough analysis of the full-cycle exergetic efficiency and CO_{2eq} intensity of the underground hydrogen (H_2) storage process, taking into account different H_2 production methods. Our primary objective is to assess these metrics across two key areas: the complete H_2 supply chain, which encompasses H_2 production, transportation, underground storage, and end-use applications, as well as the specific process of underground storage.

1. Full H_2 supply chain

A significant portion of the total exergy is consumed during the H_2 production phase. Depending on the chosen tail-gas handling approach (Scenario 1 or 2), subsurface storage and the application of H_2 at the end-use stage account for approximately 6 % and 25 % of the total exergy investment, respectively. With fuel cells' conversion efficiencies, 48–87 Mj (MJ) of electricity can be generated from 1 kg of H_2. Utilizing Eq. (1), we calculate that the maximum exergetic efficiency of the entire system, ranges from 0.07 to 0.25. This reveals that a substantial part of the invested exergy (75–93 %) is lost throughout the cycle of converting electricity to H_2 and back to electricity.

Fig. 3 illustrates the exergetic efficiency (ERoEI) in the full H_2 supply chain for different H_2 production techniques. Among these, the Partial Oxidation (POX) method emerges with the highest overall exergetic efficiency, marked at ERoEI=0.25. Since the output pressure of H_2 obtained by the POX method is higher (50 bar) compared to the other methods, less exergy is spent on the compression stage. Furthermore, integrating Carbon Capture and Storage (CCS) with any H_2 production method – resulting in so-called blue H_2 – decreases the overall exergetic efficiency. This decline is primarily due to the additional exergy required for CO_2 capture.

As previously discussed, once the exergy invested in the process is determined, its corresponding CO_2 intensity can also be calculated by considering the specific CO_2 emissions of the energy source. Fig. 4 presents the CO_2 equivalent intensity for the entire supply chain through various H_2 production methods.

The production of grey H_2 results in a significantly high level of CO_2 emissions. To mitigate this, the blue H_2 option incorporates Carbon Capture and Storage (CCS) technologies to capture the CO_2 produced during operations. However, it is important to acknowledge that not all emitted CO_2 can be captured, and part of the generated CO_2 is released. The implementation of CCS in the blue H_2 production significantly reduces the CO_2 intensity of the generated electricity by 34–76 %, as illustrated in Fig. 4. The CO_2 capture efficiency is estimated to be between 80–90 % for Steam Methane Reforming (SMR) and 90–100 % for Autothermal Reforming (ATR) and Partial Oxidation (POX) methods [53–55]. The higher capture efficiency in ATR and POX is attributed to the injection of pure oxygen (O_2) into the system, which prevents nitrogen dilution in the syngas and flue gas streams. This efficiency allows a single CCS unit to capture a large volume of emissions effectively. In contrast, the SMR method may require multiple CCS units to achieve up to 90 % capture of onsite emissions. Thus, ATR and POX methods are preferred for carbon capture due to their simpler CO_2 removal processes than the SMR method [50,51].

Our analysis further reveals that H_2 production via the POX+CCS and ATR+CCS methods exhibit, on average, 20 % lower CO_2 intensity compared to the SMR+CCS method when generating electricity. Nevertheless, the most environmentally friendly approach for electricity generation from H_2 chain is through green H_2, produced via water electrolysis, which eliminates methane (CH_4) emissions and utilizes low-carbon power sources. The CO_{2eq} intensity for this method ranges between 22.8–123 gr-CO_{2eq}/MJe. In terms of CO_2 intensity, electricity generation from blue methane (CH_4 + CCS) is comparable to green H_2, emitting nearly 2.5 times less CO_2 than the blue H_2 option. The data for the blue CH_4 route is adapted from the work of Farajzadeh et al. [23], with an adjustment to include 0–1.5 % of fugitive CH_4 emissions for consistency. Moreover, the CH_4 + CCS option also demonstrates higher exergetic efficiency compared to the H_2 supply chain, with ranging from 0.76 to 2.58 for electricity generation. This enhanced efficiency is primarily because CH_4 serves as a primary energy source, with relatively low production costs from an exergy perspective [23].

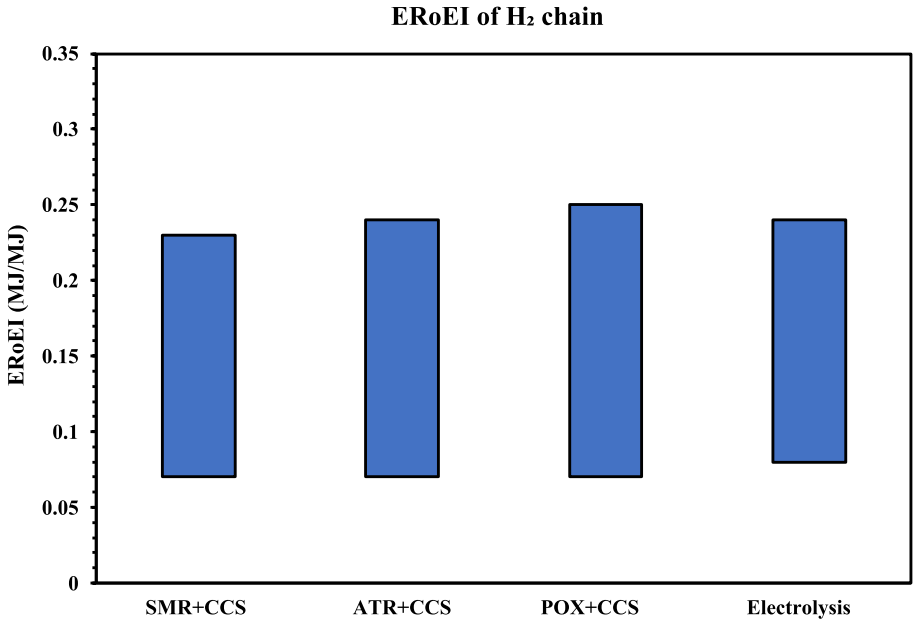

Fig. 3. The exergetic efficiency (ERoEI) of the full $H_{2\ \text{supply chain}}$ shown in Fig. 1 including H_2 production, underground storage, and application processes considering different H_2 production methods.

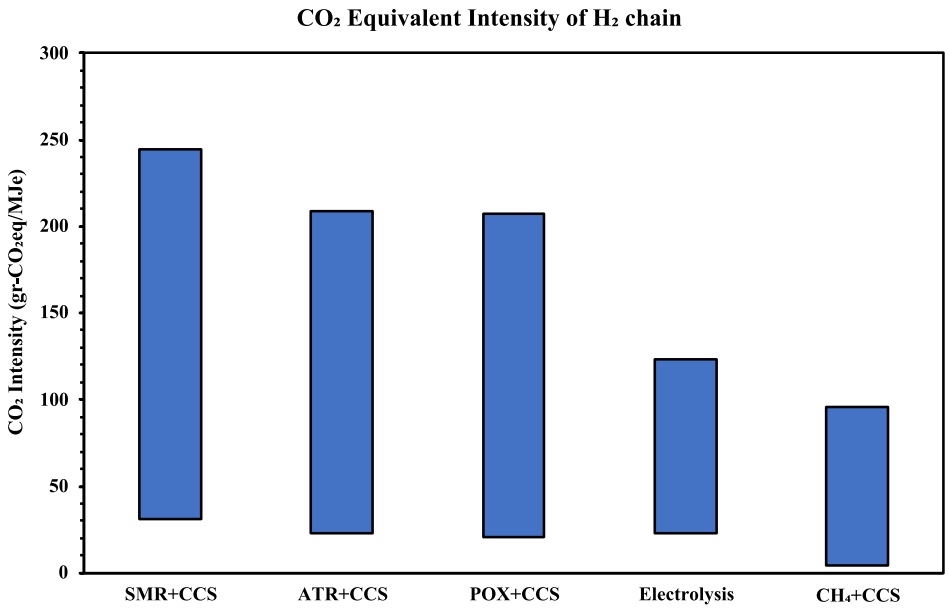

Fig. 4. CO_{2eq} Intensity of the full H_2 supply chain including H_2 production, underground storage, and application processes for different H_2 production methods and considering CO_2, CH_4 and H_2 emissions. Results are compared with the CH_4 + CCS option.

Fig. 4 incorporates the impact of fugitive methane (CH_4) and hydrogen (H_2) emissions on the system's CO_{2eq} intensity, applying Eq. (3) for calculation. Despite CH_4 leaks occurring less frequently than H_2 within the system, the global warming potential (GWP) of CH_4 is significantly higher, leading to a greater effect on greenhouse gas emissions. Specifically, a fugitive emission rate of 1.5 % for CH_4 can augment the CO_{2eq} intensity of electricity generation by 11–25 %. Should the CH_4 leakage rate escalate to 3 %, this increase in total CO_{2eq} intensity could range from 24-49 % over a 100-year period. Additionally, the impact of CH_4 leakage is also evaluated over shorter durations, such as a 20-year period in some studies, where the GWP of CH_4 is recognized to be 86 [45]. In such a scenario, 1.5 % CH_4 leakage could elevate the CO_{2eq} intensity by 48–69 %. In comparison, leakage rates of 3.5–9 % H_2 in the system contribute to an increase the total CO_{2eq} intensity by 4–20 gr-CO_{2eq}/MJe, translating to an increase of 5–23 % over a 100-year period.

Fig. 5 and Fig. 6 present the average contribution of the invested exergy and the corresponding specific CO_2 emissions with blue and green H_2 production methods, respectively. In each case, the predominant share of total exergy is allocated to the H_2 production phase, comprising 56 % for blue H_2 and 67 % for green H_2. The elements of subsurface storage and electricity generation are responsible for about 6 % and 25 % of the overall exergy investment, respectively. Moreover, within the blue H_2 pathway, 13 % of the exergy is expended during the CO_2 capture process. A similar contribution is observed for the CO_2 footprint of the system. The emission from the H_2 production stage accounts for a big portion of the total emission in both green and blue H_2 options, with 76 % and 84 %, respectively. The CCS stage in the blue H_2 option emits 13 % of the total CO_2 emissions. Operations involved in subsurface storage, including compression, separation, and handling of tail-gas, are estimated to contribute 6–7 % of the emissions. The analysis also indicates that transportation components emit a comparatively small amount of CO_2, ranging from 1-2 %.

2. Underground Storage Process

As depicted in Fig. 2, the underground hydrogen storage (UHS) process is composed of three primary components: injection, gas processing, and tail-gas handling. The term "loss" refers to the amount of H_2 that remains trapped within the reservoir due to either mixing or hydrodynamic/geochemical interactions. This retained H_2 reduces the exergy return but does not contribute to H_2 emissions. Eq. (1) illustrates how H_2 loss within the reservoir directly impact on the Exergy Return on Exergy Invested (ERoEI), indicating that any reduction in exergy return

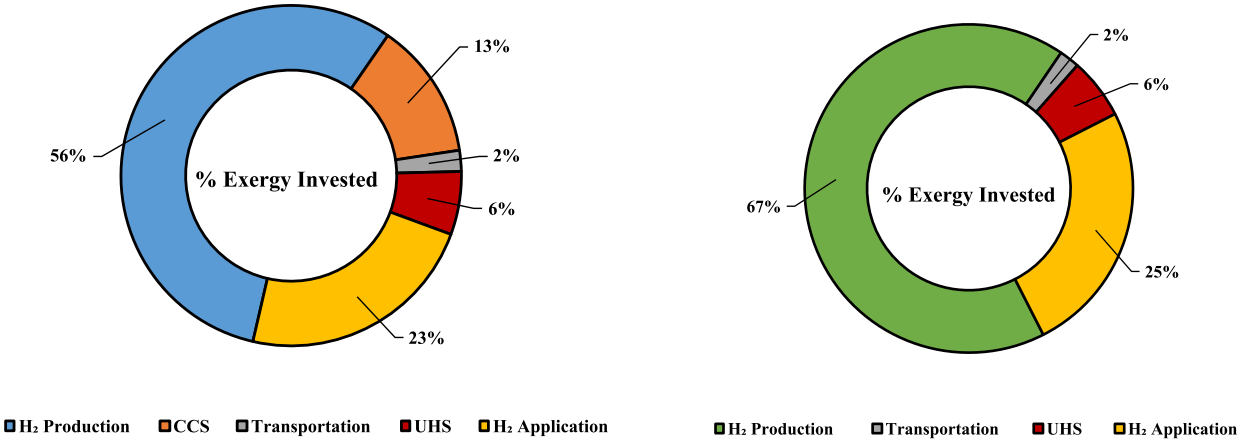

Fig. 5. Fraction of the exergy investment with blue (left) and green H_2 (right) production methods.

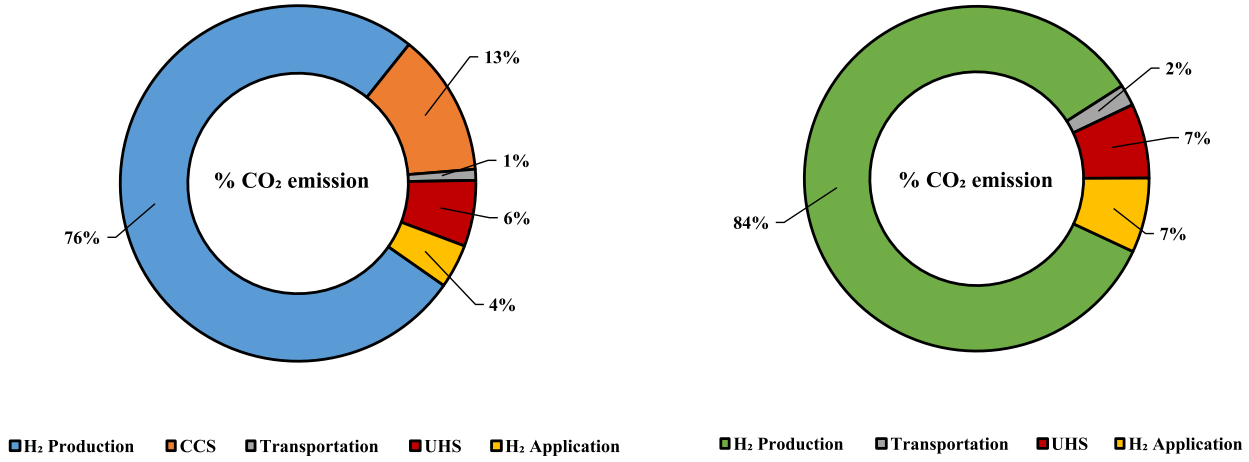

Fig. 6. Fraction of the CO_2 emission with blue (left) and green H_2 (right) production methods.

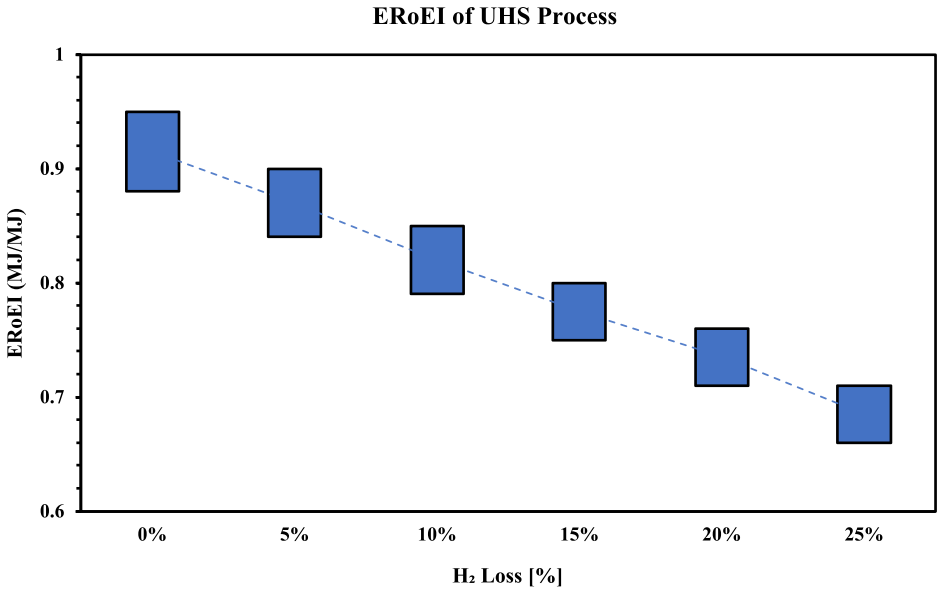

Fig. 7. Exergy return on the exergy investment (ERoEI) as a function of H_2 loss for the UHS process.

due to H_2 loss leads to a decrease in ERoEI. The exergetic efficiency for the UHS component is estimated to be between 0.72 and 0.92.

Fig. 7 further elucidates the influence of H_2 loss on the exergetic efficiency of the UHS process. It is evident that the exergetic efficiency diminishes as H_2 loss increases. For instance, the average ERoEI decreases from 0.91 – with no H_2 loss (equating to 100 % H_2 recovery factor) to 0.78 for a 15 % H_2 loss (equating to 85 % H_2 recovery factor).

Corresponding to the exergetic efficiency, the CO_{2eq} intensity of the UHS is calculated to range 1.46–4.56 gr-CO_{2eq}/MJ, under the assumption that low-carbon energy sources, such as wind power, are utilized for all subsurface operations. Studies indicate that surface operations typically experience a 1–2 % H_2 leakage rate (Table 5).

Fig. 8 shows the relationship between CO_2 intensity and different H_2 leak rates within UHS process. The results indicate that H_2 leak has a considerable impact on the CO_{2eq} intensity, which rises significantly with higher leakage rates. For example, the CO_{2eq} intensity increases from 2.4 gr-CO_{2eq}/MJ to 14 gr-CO_{2eq}/MJ as the H_2 leak rate increases from 1 % to 10 %.

The choice of tail gas handling does not have a significant impact on the exergetic efficiency of the overall system. Scenario 2, i.e., which involves export of CH_4 to a gas power plant, yields a slightly higher exergy gain but also a slightly increased CO_2 intensity compared to Scenario 1, where CH_4 is re-injected into the storage reservoir. The reason for this is that in Scenario 2 the conversion of the chemical exergy of CH_4 into electricity results in a larger exergy gain; however, this conversion process is accompanied by additional CO_2, which needs to be captured. Fig. 9 and Fig. 10 present the average distribution of the exergy investment and the unit CO_2 emitted over the scenarios in a comparative manner. In both scenarios, the injection phase, particularly the compression stage, accounts for the largest portion of exergy consumption, with figures at 49 % and 48 %, respectively. The gas processing segment, which includes separation, is the second-largest contributor, with 42–44 %. When comparing scenarios, in Scenario 2 (exporting CH_4 to gas power plant and capturing generated CO_2 from combustion) CCS process demands a slightly higher exergy investment than in Scenario 1 (reinjection of CH_4 back into reservoir). Furthermore, larger exergy investment corresponds to a larger fraction of CO_2 emission. Consequently, the injection stage produces the highest CO_2 emission in Scenario 1. Nonetheless, despite the lower exergetic cost of tail-gas handling in Scenario 2, this stage accounts for 41 % of the total CO_2 emissions. This arises from the CCS process and combustion of the exported CH_4.

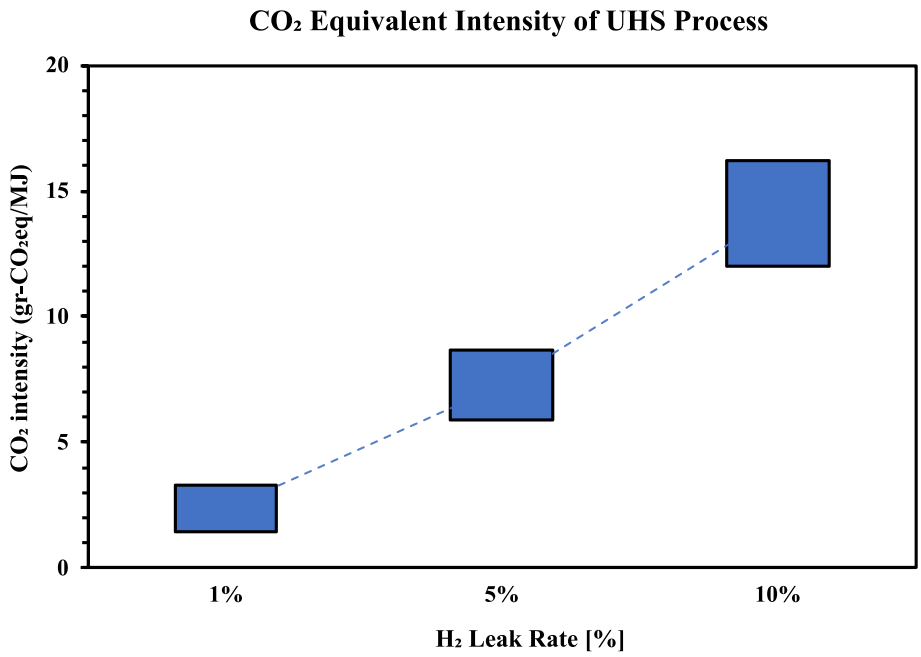

Fig. 8. Impact of H_2 leak rate on CO_{2eq} intensity in UHS process.

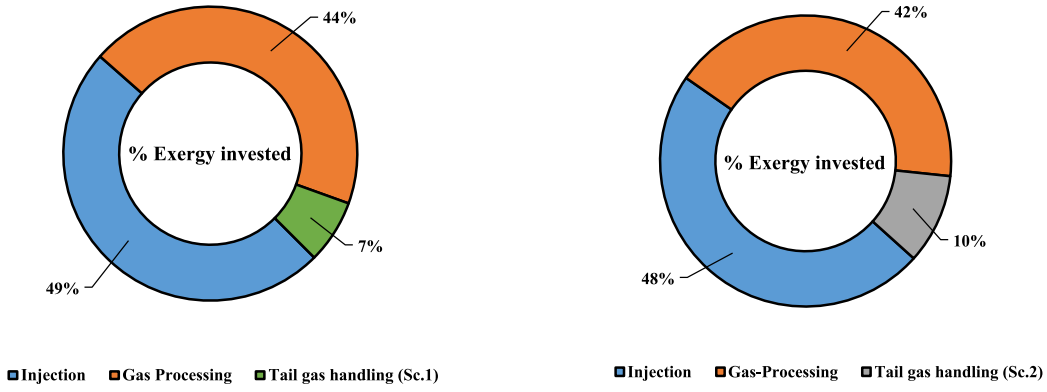

Fig. 9. Fraction of exergy investment in the UHS process with different tail-gas handling scenarios (referring to Fig. 2).

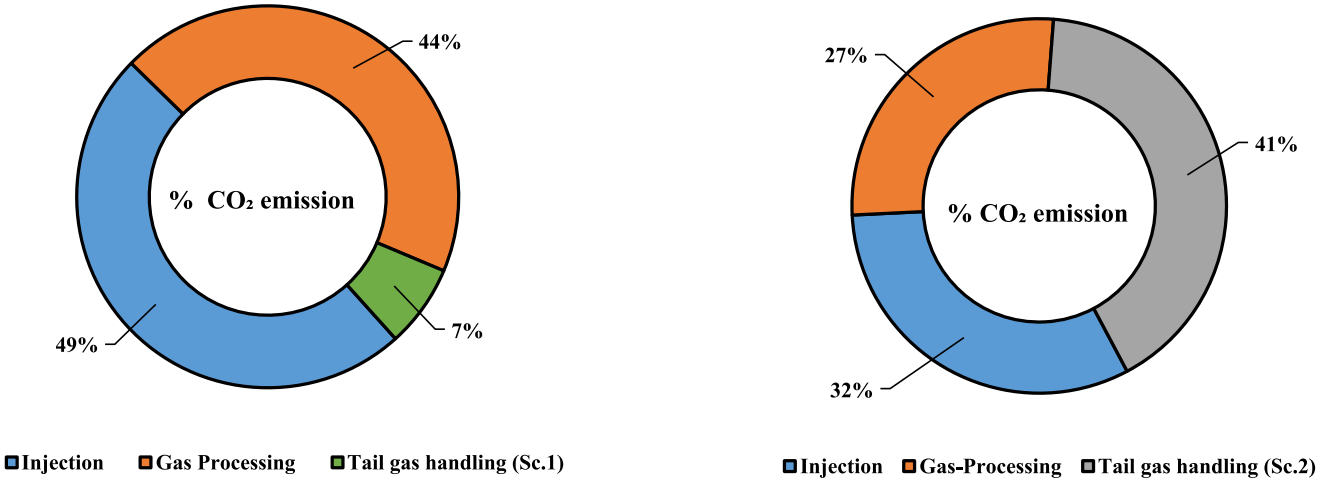

Fig. 10. Fraction of the CO_2 emission in the UHS process with different tail-gas handling scenarios (referring to Fig. 2).

Conclusions

In this study, the concept of exergy-return on exergy-investment (ERoEI) is used to estimate the exergetic efficiency of electricity generation via underground H_2 storage process, examining different H_2 production methods. Through detailed analysis, the ERoEI and CO_2 equivalent intensity (gr-CO_{2eq}/MJe) are calculated for the entire H_2 supply chain, including the underground storage option. Based on the system's assumptions and defined boundaries, we draw the following conclusions:

- The Partial Oxidation (POX) and Autothermal Reforming (ATR) methods exhibit the highest exergetic efficiency (ERoEI) throughout the process. These methods also offer lower CO_2 intensities in comparison to the Steam Methane Reforming (SMR) method.
- Although electrolysis using renewable power being an energy intensive process, it has the lowest CO_2 intensity for electricity generation among the H_2 production methods.
- H_2 loss at any stage of the process significantly reduces ERoEI of the system.
- Integrating a CO_2 capture plant during the production phase of blue H_2 significantly reduces the CO_2 intensity of the entire supply chain, by around halving it, albeit at the expense of reduced exergetic efficiency (ERoEI).
- The blue methane (CH_4 + CCS) option demonstrates higher exergetic efficiency and lower CO_2 intensity compared to the blue H_2 option. However, blue H_2 is a promising route for electricity generation, which can help decarbonize the energy sector.
- The inclusion of CH_4 emissions increases the overall CO_2 equivalent intensity of blue H_2, with the magnitude depending on the leakage rate. For 1.5 % CH_4 leakage rate, the CO_2 intensity increases by 25 % (100 years' time frame).
- The exergetic efficiency of the underground hydrogen storage process is calculated in the range of 72–92 %. The largest exergy investments are consumed for injection components.
- Utilizing low-carbon power sources in subsurface storage operations contributes minimally to CO_2 emissions, estimated between 1.46–4.56 gr-CO_{2eq}/MJ.

CRediT authorship contribution statement

Boyukagha Baghirov: Writing – original draft, Visualization, Methodology, Investigation, Conceptualization, Formal analysis. **Denis Voskov:** Writing – review & editing, Supervision. **Rouhi Farajzadeh:** Writing – review & editing, Supervision, Project administration, Conceptualization, Methodology, Writing – original draft.

Declaration of competing interest

The authors declare that they have no known competing financial interests or personal relationships that could have appeared to influence the work reported in this paper.

Data availability

No data was used for the research described in the article.

Acknowledgement

The authors thank Shell Global Solutions International for granting permission to publish this paper. The authors also thank Prof.dr. Hadi Hajibeygi for reviewing the initial draft of this manuscript.

References

[1] *DNV Technical Report: ENERGY TRANSITION OUTLOOK 2022.*
[2] Gielen D, et al. The role of renewable energy in the global energy transformation. Energ Strat Rev 2019;24:38–50.
[3] Muhammed NS, et al. A review on underground hydrogen storage: Insight into geological sites, influencing factors and future outlook. Energy Rep 2022;8:461–99.
[4] Heinemann N, et al. Enabling large-scale hydrogen storage in porous media – the scientific challenges. Energ Environ Sci 2021;14(2):853–64.
[5] Ji M, Wang J. Review and comparison of various hydrogen production methods based on costs and life cycle impact assessment indicators. Int J Hydrogen Energy 2021;46(78):38612–35.
[6] Liu W, et al. Trends and future challenges in hydrogen production and storage research. Environ Sci Pollut Res 2020;27(25):31092–104.
[7] Böttcher N, et al. Thermo-mechanical investigation of salt caverns for short-term hydrogen storage. Environ Earth Sci 2017;76(3):98.
[8] Tarkowski R, Czapowski G. Salt domes in Poland – Potential sites for hydrogen storage in caverns. Int J Hydrogen Energy 2018;43(46):21414–27.
[9] Caglayan DG, et al. Technical potential of salt caverns for hydrogen storage in Europe. Int J Hydrogen Energy 2020;45(11):6793–805.
[10] Sainz-Garcia A, et al. Assessment of feasible strategies for seasonal underground hydrogen storage in a saline aquifer. Int J Hydrogen Energy 2017;42(26):16657–66.
[11] Heinemann N, et al. Hydrogen storage in porous geological formations – onshore play opportunities in the midland valley (Scotland, UK). Int J Hydrogen Energy 2018;43(45):20861–74.
[12] Luboń K, Tarkowski R. Numerical simulation of hydrogen injection and withdrawal to and from a deep aquifer in NW Poland. Int J Hydrogen Energy 2020;45(3):2068–83.
[13] Amid A, Mignard D, Wilkinson M. Seasonal storage of hydrogen in a depleted natural gas reservoir. Int J Hydrogen Energy 2016;41(12):5549–58.
[14] Lemieux A, Sharp K, Shkarupin A. Preliminary assessment of underground hydrogen storage sites in Ontario. *Canada* International Journal of Hydrogen Energy 2019;44(29):15193–204.
[15] Bo Z, et al. Accounting Green and Blue Hydrogen in a Net Cash Flow Model for Techno-Economic Assessment on Underground Hydrogen Storage in Australia. In *Asia Pacific Unconventional Resources Symposium*. 2023.
[16] Abreu JF, et al. Carbon net zero transition: A case study of hydrogen storage in offshore salt cavern. J Storage Mater 2023;62:106818.
[17] Lucas van Cappellen HC, Rooijers F. CE Delft Report. Feasibility study into blue hydrogen. Technical, Economic & Sustainability Analysis 2018.
[18] Ozcan H, Dincer I. Energy and exergy analyses of a solar based hydrogen production and compression system. Int J Hydrogen Energy 2017;42(33):21414–28.
[19] Calderón M, et al. Evaluation of a hybrid photovoltaic-wind system with hydrogen storage performance using exergy analysis. Int J Hydrogen Energy 2011;36(10):5751–62.
[20] Khosravi A, et al. Energy, exergy and economic analysis of a hybrid renewable energy with hydrogen storage system. Energy 2018;148:1087–102.
[21] Al-Zareer, M., I. Dincer, and M.A. Rosen, *Transient Energy and Exergy Analyses of a Multistage Hydrogen Compression and Storage System.* Chemical Engineering & Technology, 2018. 41(8): p. 1594-n/1603.
[22] Neelis ML, van der Kooi HJ, Geerlings JJC. Exergetic life cycle analysis of hydrogen production and storage systems for automotive applications. Int J Hydrogen Energy 2004;29(5):537–45.
[23] Farajzadeh R, et al. Exergy Return on Exergy Investment and CO2 Intensity of the Underground Biomethanation Process. ACS Sustain Chem Eng 2022;10(31):10318–26.
[24] Arias Pérez A, Vogt T. Life cycle assessment of conversion processes for the large-scale underground storage of electricity from renewables in Europe. EPJ Web of Conferences 2014;79.
[25] Bhandari R, Trudewind CA, Zapp P. Life cycle assessment of hydrogen production via electrolysis – a review. J Clean Prod 2014;85:151–63.
[26] Timmerberg S, Kaltschmitt M, Finkbeiner M. Hydrogen and hydrogen-derived fuels through methane decomposition of natural gas – GHG emissions and costs. Energy Conversion and Management: X 2020;7:100043.
[27] Kubilay Karayel G, Javani N, Dincer I. A comprehensive assessment of energy storage options for green hydrogen. Energ Conver Manage 2023;291:117311.
[28] Bicer Y, et al. Comparative life cycle assessment of various ammonia production methods. J Clean Prod 2016;135:1379–95.
[29] Nikolaidis P, Poullikkas A. A comparative overview of hydrogen production processes. Renew Sustain Energy Rev 2017;67:597–611.
[30] Al-Qahtani A, et al. Uncovering the true cost of hydrogen production routes using life cycle monetisation. Appl Energy 2021;281:115958.
[31] Kothari R, Buddhi D, Sawhney RL. Comparison of environmental and economic aspects of various hydrogen production methods. Renew Sustain Energy Rev 2008;12(2):553–63.
[32] Al-Ghussain L, et al. Integrated assessment of green hydrogen production in California: Life cycle Greenhouse gas Emissions, Techno-Economic Feasibility, and resource variability. Energ Conver Manage 2024;311:118514.
[33] Rosen, M., *Enhancing Ecological and Environmental Understanding with Exergy: Concepts and Methods.* Proceedings of the 4th IASME/WSEAS Int. Conference on Water Resources, 2009.

[34] Huang W, et al. Exergy-environment assessment for energy system: Distinguish the internal and total exergy loss, and modify the contribution of utility. Energ Conver Manage 2022;251:114975.
[35] Farajzadeh R. Sustainable production of hydrocarbon fields guided by full-cycle exergy analysis. J Pet Sci Eng 2019;181:106204.
[36] Szargut J. Analysis of cumulative exergy consumption. Int J Energy Res 1987;11 (4):541–7.
[37] Eftekhari AA, Van Der Kooi H, Bruining H. Exergy analysis of underground coal gasification with simultaneous storage of carbon dioxide. Energy 2012;45(1): 729–45.
[38] Hassan AM, et al. Exergy return on exergy investment analysis of natural-polymer (Guar-Arabic gum) enhanced oil recovery process. Energy 2019;181:162–72.
[39] Farajzadeh R, et al. Life-cycle production optimization of hydrocarbon fields: thermoeconomics perspective. Sustainable Energy Fuels 2019;3(11):3050–60.
[40] Farajzadeh R, et al. On the sustainability of CO2 storage through CO2 – Enhanced oil recovery. Appl Energy 2020;261:114467.
[41] Dröge, R., N.E. Ligterink, and W.W.R. Koch, *TNO Report: Update of the Netherlands list of fuels in 2021*. 2021.
[42] *WNA Report Comparison of Lifecycle Greenhouse Gas Emissions of Various Electricity Generation Sources*. 2011.
[43] Budsberg E, et al. Ethanologens vs. acetogens: Environmental impacts of two ethanol fermentation pathways. Biomass Bioenergy 2015;83:23–31.
[44] Spath PL, Mann MK. Life Cycle Assessment of Hydrogen Production via Natural Gas Steam Reforming. National Renewable Energy Laboratory; 2001.
[45] Howarth RW, Jacobson MZ. How green is blue hydrogen? Energy Sci Eng 2021;9 (10):1676–87.
[46] Ocko IB, Hamburg SP. Climate consequences of hydrogen emissions. Atmos Chem Phys 2022;22(14):9349–68.
[47] *Report. Shell Global. Tackling Methane Emissions*. Available from: https://www.shell.com/energy-and-innovation/natural-gas/methane-emissions.html.
[48] OGCI. *Methane Intensity Target*. Available from: https://www.ogci.com/methane-emissions/methane-intensity-target.
[49] ZHIYUAN FAN, H.S., AMAR BHARDWAJ, ANNE-SOPHIE CORBEAU, KATHRYN, A. C. LONGOBARDI, ANN-KATHRIN MERZ, DR. CALEB M. WOODALL, MAHAK, and S.O.-S. AGRAWAL, DR. JULIO FRIEDMANN, *HYDROGEN LEAKAGE: A POTENTIAL RISK FOR THE HYDROGEN ECONOMY*. 2022, COLUMBIA SIPA, Center on Global Energy Policy.
[50] IPCC, *Climate Change 2013: The Physical Science Basis*, T.F. Stocker, D. Qin, G.-K. Plattner, M. Tignor, S.K. Allen, J. Boschung, A. Nauels, Y. Xia, V. Bex and P.M. Midgley Editor. 2013.
[51] Warwick NJ, et al. Atmospheric composition and climate impacts of a future hydrogen economy. Atmos Chem Phys 2023;23(20):13451–67.
[52] Sand M, et al. A multi-model assessment of the Global Warming Potential of hydrogen. Communications Earth & Environment 2023;4(1):203.
[53] *IEA Technical Report: Low-Carbon Hydrogen from Natural Gas: Global Roadmap*. 2022.
[54] Khojasteh Salkuyeh Y, Saville BA, MacLean HL. Techno-economic analysis and life cycle assessment of hydrogen production from natural gas using current and emerging technologies. Int J Hydrogen Energy 2017;42(30):18894–909.
[55] Oni AO, et al. Comparative assessment of blue hydrogen from steam methane reforming, autothermal reforming, and natural gas decomposition technologies for natural gas-producing regions. Energ Conver Manage 2022;254:115245.
[56] *Gaffney Cline Report. Underground Hydrogen Storage (UHS)*. 2022.
[57] Morris DR, Szargut J. Standard chemical exergy of some elements and compounds on the planet earth. Energy 1986;11(8):733–55.
[58] Geuzebroek FH, et al. Exergy analysis of alkanolamine-based CO2 removal unit with AspenPlus. Energy 2004;29(9):1241–8.
[59] Ferrara G, et al. Exergetic and exergoeconomic analysis of post-combustion CO2 capture using MEA-solvent chemical absorption. Energy 2017;130:113–28.
[60] Simoes SG, et al. Water availability and water usage solutions for electrolysis in hydrogen production. J Clean Prod 2021;315:128124.
[61] Rao P, et al. Energy considerations associated with increased adoption of seawater desalination in the United States. Desalination 2018;445:213–24.
[62] Miller, J.E., *Review of Water Resources and Desalination Technologies*. 2003: United States.
[63] Shahabi MP, McHugh A, Ho G. Environmental and economic assessment of beach well intake versus open intake for seawater reverse osmosis desalination. Desalination 2015;357:259–66.
[64] El-Shafie MI, Kambara S, Hayakawa Y. Hydrogen Production Technologies Overview. Journal of Power and Energy Engineering 2019;7:107–54.
[65] Holladay JD, et al. An overview of hydrogen production technologies. Catal Today 2009;139(4):244–60.
[66] Hodges A, et al. A high-performance capillary-fed electrolysis cell promises more cost-competitive renewable hydrogen. Nat Commun 2022;13(1):1304.
[67] Dincer I, Acar C. Review and evaluation of hydrogen production methods for better sustainability. Int J Hydrogen Energy 2015;40(34):11094–111.
[68] *CoolProp Software*. Available from: http://www.coolprop.org/.
[69] Ipieca. *Compressors*. 2022; Available from: https://www.ipieca.org/resources/energy-efficiency-solutions/compressors-2022.
[70] Holloway Seth; Horton W. Travis; Groll Eckhard A.; Sherman Dan; and Albertin, M., *Experimental Performance of a Prototype Carbon Dioxide Compressor*, in *International Compressor Engineering Conference. Paper 2037*. 2010.
[71] Linquip-Technews. *Efficiency of Electric Motor: A Simple Guide*. 2021; Available from: https://www.linquip.com/blog/efficiency-of-electric-motor/.
[72] Linquip-Technews. *Efficiency of Wind Turbines*. 2022; Available from: https://www.linquip.com/blog/efficiency-of-wind-turbines/.
[73] Witkowski A, et al. Comprehensive analysis of hydrogen compression and pipeline transportation from thermodynamics and safety aspects. Energy 2017;141: 2508–18.
[74] Eftekhari A and R. Farajzadeh., *Environmental and Technical Advantages and Bottlenecks of Carbon Dioxide Capture and Storage from a Thermodynamic Perspective.*, in *The 35th International Conference on Efficiency, Cost, Optimization, Simulation and Environmental Impact of Energy Systems 2022*. 2022.
[75] Liu Z, et al. Simulation and energy consumption comparison of gas purification system based on elevated temperature pressure swing adsorption in ammonia synthetic system. Adsorption 2020;26(7):1239–52.
[76] Paturska A, Repele M, Bazbauers G. Economic Assessment of Biomethane Supply System based on Natural Gas Infrastructure. Energy Procedia 2015;72:71–8.
[77] Uehara, I., *Energy Carriers And Conversion Systems With Emphasis On Hydrogen - Volume 1*. SEPARATION AND PURIFICATION OF HYDROGEN. Encyclopedia of Life Support Systems (EOLSS).
[78] Du Z, et al. A Review of Hydrogen Purification Technologies for Fuel Cell Vehicles. Catalysts 2021;11. https://doi.org/10.3390/catal11030393.
[79] *US Department of Energy (DOE). Fuel Cells Fact Sheet.* . 2015; Available from: https://www.energy.gov/sites/prod/files/2015/11/f27/fcto_fuel_cells_fact_sheet.pdf.
[80] Schorer L, Schmitz S, Weber A. Membrane based purification of hydrogen system (MEMPHYS). Int J Hydrogen Energy 2019;44(25):12708–14.
[81] Derwent R, et al. Global environmental impacts of the hydrogen economy. International Journal of Nuclear Hydrogen Production and Applications 2006;1(1): 57–67.